Effect Of Interfiber Spacing On The High Temperature Deformation Of Al-Al_3Ni Composites

by Harry Colson Lewis

Supervisor: Dr. J. Wulff

17 May 1968

EFFECT OF INTERFIBER SPACING ON THE HIGH TEMPERATURE DEFORMATION OF Al-Al_3Ni COMPOSITES

by

HARRY COLSON LEWIS

LIEUTENANT, UNITED STATES NAVY

B.S., United States Naval Academy

(1960)

Submitted in Partial Fulfillment of the

Requirements for the Degree of

Naval Engineer and the Degree of

Master of Science in Mechanical Engineering

at the

MASSACHUSETTS INSTITUTE OF TECHNOLOGY

May, 1968

Effect of Interfiber Spacing on the High Temperature Deformation of Al-Al_3Ni Composites

Harry Colson Lewis

Submitted to the Department of Mechanical Engineering and the Department of Naval Architecture and Marine Engineering on 17 May 1968 in partial fulfillment of the requirements for the Master of Science degree in Mechanical Engineering and the Professional Degree, Naval Engineer.

ABSTRACT

To investigate the formability and high temperature tensile strength of Al-Al_3Ni fiber composites, directionally solidified tensile specimens were grown in a verticle run furnace. The specimens were grown at four growth rates ranging from 3.5 to 9.4 cm/hr, and two nickel weight fractions, 6.13 and 6.2 wt % Ni. Test temperatures ranged from room temperature to 500°C. The results showed a steep decrease in tensile strength with increasing temperature. Above 250°C, however, the tensile strengths leveled off. The 6.2 wt % Ni composite showed better strength than the 6.13 wt % Ni composite. The tensile strengths increased with increasing growth rate from 3.5 to 5.2 cm/hr. At yet higher growth rates, it was found that microstructural defects were more prevalent than at the lower rates and the strengths decreased. The defects encountered were fiber depleted grain boundaries and banded areas of misaligned fibers. When both defects occurred simultaneously, the specimen failed in matrix shear with a low ultimate tensile strength. The percentage elongation of the samples was generally from 1 to 3% before the ultimate strength was reached. For those samples that had a sufficiently defective microstructure, elongation was extensive after yield and occurred uniformly over the gage length. Multiple shear planes were aligned parallel to the eventual failure plane. Strain rate sensitivity tests on specimens that showed unusual elongation after yield resulted in a low strain rate sensitivity index that decreased with increasing % elongation.

Thesis Supervisor: John Wulff

Title: Professor of Metallurgy

TABLE OF CONTENTS

LIST OF FIGURES

ACKNOWLEDGMENTS

This project was sponsored by the United States Air Force Contract No. AF49(638)-1463. The author wishes to thank Dr. J. Wulff for the use of laboratory space and equipment during the conduct of the research. Special acknowledgment is made for the technical assistance given the author by Dr. L. Shepard, Dr. T. Courtney, Messrs. P. Heitman, and G. Garmong of the Department of Metallurgy and Materials Science at M.I.T.

I INTRODUCTION

In recent years considerable study has been devoted to the field of unidirectional solidification of eutectics. Hunt and Jackson[1,2] have presented a theory whereby a eutectic type microstructure will result over almost the entire composition range. A fiber type microstructure will result, given the proper purity, solidification rate, and temperature gradient at the liquid-solid interface. Mollard and Flemings[3] concluded that it is possible to maintain a plane solidification front in alloys far from the eutectic composition. However, small changes in the interface velocity have a significant effect of fluctuations in the solid concentration. They also concluded that the temperature at the liquid-solid interface is the eutectic temperature regardless of the composition.

The result of unidirectional motion of the planar liquid-solid interface is a eutectic microstructure which consists of two phases aligned parallel to one another. The micromorphology produced is either parallel lamellae of alternating phase, or long thin parallel rods of one phase in a continuous matrix of the other. Impurities cause a breakdown in the planar interface, resulting in a eutectic colony microstructure;[4] however, in a purity

controlled eutectic, the formation of plates or rods has been shown to depend on the solidification rate.[5,6]

In their study of the Al-Al_3Ni eutectic, Lemkey, Hertzberg, and Ford[6,7] concluded that the unidirectionally solidified eutectic is normally of the rod type micromorphology, with the inter-rod spacing inversely proportional to the square root of the solidification rate. The Al_3Ni eutectic was found to have a critical solidification rate at 2.6 cm/hr. Below this rate the eutectic would form into platelets rather than cylindrical rods. Parallel eutectic growth was obtained from melts containing from 5.7 to 6.4 wt % Ni. The actual eutectic composition, however, was determined to be 6.18 + 0.05 wt % Ni.

The eutectic rods were shown to behave as whisker reinforcement to the matrix. Room temperature tensile strengths of the composite have been averaged at 40000 psi, whereas the tensile strengths of the as cast eutectic and matrix material were averaged at 13000 and 8000 psi respectively.[8]

Specimens directionally solidified at rates from 1.1 to 28.7 cm/hr were tested at room temperature.[7] Of twenty-one samples tested, sixteen failed at the shoulder of the gage section. It was thought that tool markings on the specimens caused the scatter in the data. However, on examining the microstructure of the test samples, it

was found that two microstructural defects were the primary cause of the scatter. The most serious defect was a narrow annular band perpendicular to the growth direction in which the matrix was depleted of eutectic whiskers. Failure always occurred at these annular bands. The second defect was again a depleted zone of whiskers in the matrix parallel to the growth direction. (Figure I)

The test results showed a definite increase in room temperature tensile strength with increasing solidification rate. As the fibers became thinner and more closely spaced, the strength increased. The measured interfiber spacing, λ (microns), was found to vary with the growth rate, R (cm/hr), according to the relation:

$$\lambda = 4.55R^{-\frac{1}{2}} + 0.2$$

Kelly and Davies[11] postulated that at small angles of misorientation of the fibers with respect to the tensile axis the tensile stress transferred from the matrix to the fibers would decrease. The resulting tensile strength would increase with the inverse square of the cosine of the angle of misorientation. At the critical angle, however, the matrix will fail in shear. With increasing temperature, the matrix shear strength generally decreases more rapidly than the fiber strength, thus decreasing the critical angle. This increases the tendency for shear failure with increasing temperature in

samples with misaligned fibers. George, Ford, and Salkind[9] examined the room temperature anisotropic behavior of the Al-Al_3Ni composite by varying the tensile axis with respect to the fiber orientation. They concluded that the whiskers provided considerable strength to the Al matrix even when the tensile load was perpendicular to the growth axis. Specimens were tested with the fiber orientation aligned at 0, 25, 45, and 90 degrees to the tensile axis. Deformation was primarily by shear of the matrix, the fibers providing interference to most slip systems. With the rod type whiskers, grown at 3.25 cm/hr, the tensile strength decreased from over 45,000 psi at 0 degrees orientation to an average of 10000 psi at 90 degrees fiber orientation. From the experimental findings, the critical angle of fiber misorientation is about 10 degrees for the rod type fiber morphology.

Bayles, Ford, and Salkind[10] have investigated the effect of long periods at high temperature on the microstructure and tensile strength at room temperature of the Al-Al_3Ni composite. It was found that the composite retained its room temperature tensile strength after heat treatment in spite of a mild coarsening of the microstructure. This coarsening of microstructure was found to occur at high temperatures close to the eutectic temperature, and it varied with the initial rod density.

They concluded that the driving force for coarsening is the lowering of interfacial energy by lowering the interfacial area of the two phases. Although the interfiber spacing increased after heat treatment, the tensile strength depends only on the fiber strength and the volume fraction of fibers which did not change.

This investigation was initiated to determine the effect of interfiber spacing on the tensile strength characteristics of Al_3Ni fiber reinforced aluminum, tested at elevated temperatures.

II EXPERIMENTAL PROCEDURES

A. MELTING

Three separate melts were made in a graphite crucible in air with an induction furnace. Two three pound charges of 99.999% pure aluminum and 99.99% pure nickel were measured for a resultant 6.13 wt % Ni alloy. The third three pound charge was measured for an alloy of 6.2 wt % Ni. After melting, the material was held at approximately 250°C superheat for fifteen minutes to allow thorough mixing by convection. In addition the melts were stirred and impurities skimmed off the melt with a graphite rod during the superheat period. The melts were then poured into a carbon mold which had been preheated to 800°C and baked for three hours. The cast ingots from the mold measured nine inches long by one-half inch in diameter. The cast ingots were essentially oxide and hydrogen free.

B. PREPARATION OF INGOTS FOR DIRECTIONAL SOLIDIFICATION

The ingots were turned on a lathe to remove surface imperfections and then heat treated for two hours at 560°C. The heat treated ingots were then swaged to a diameter of 0.241 inches. It was found that without the two hour heat treatment after machining the cast ingots would develop surface cracks after two swage passes.

The swaged rods were cut into 6.5 inch lengths and cleaned with a 1 pct solution of hydroflouric acid in

water. The rods were then ready for directional solidification.

C. DIRECTIONAL SOLIDIFICATION

Four solidification rates were utilized; 3.5, 5.2, 6.9, and 9.4 cm/hr. Four rods in a carbon boat were raised to 700°C in an argon atmosphere. When the resistance source and boat were at temperature, a cold water heat sink at the base of the boat was turned on. The chill system provided a temperature gradient of from 20° to 30°C/cm across the liquid-solid interface. After waiting fifteen minutes to allow the temperatures to stabilize, the resistance furnace was raised vertically at the preset speed. Solidification commenced at the same rate as furnace travel. (See Appendix B for furnace control details)

D. TENSILE TESTING

It was found that fiber orientation was considerably misaligned at the bottom and top of the directionally solidified rods. Therefore 3/4 inch was cut off the top and bottom of each six inch rod. Two tensile specimens, standard 0.250 inch diameter, 1 inch gage length, were machined from the remaining rod. $\frac{1}{4}$"X20 threads were machined for the grip ends.

Tensile testing was done on an Instron tensile machine with the 1000 lbs load cell. A twelve inch cylindrical clamshell-type resistance furnace was separately mounted,

surrounding the test specimen. The furnace provided a uniform temperature zone of two inches over the sample which was constant to ± 1°C. (See Appendix B for tensile test furnace details)

Specimens of each of the four growth rates and the two weight percent compositions were tested at a crosshead speed of 0.01 "/min, at room temperature (22°C), 250°C, 375°C, and 500°C. Three specimens at the 500°C temperature exhibited considerably larger elongations than had been previously observed. For two of these specimens the crosshead speed was reduced to 0.0002 "/min and then increased back to 0.01 "/min twice during the course of the test. From the load versus elongation data obtained, strain rate sensitivity exponents were calculated from the relation

$$n = \frac{d \ln \sigma}{d \ln \dot{\varepsilon}}$$

where σ is the true stress, and $\dot{\varepsilon}$ is the true strain rate.

E. EVALUATION OF DATA

All the samples tested at 250°C were mounted in bakelite to examine their microstructures at the fracture. The three samples that showed unusual elongation at 500°C and one that did not were also examined. All results and observations, including ultimate tensile strength, percent elongation at ultimate tensile strength, strain rate sensitivity of those samples tested, type of fracture and microstructural phenomena are tabulated in Appendix A.

III RESULTS

The directional solidification of 6.13 and 6.2 wt % Ni composites resulted in complete parallel alignment of the fibers at only the 5.2 cm/hr growth rate. The other growth rates resulted in microstructural defects as shown in Figures I and II. The first of the two types of defects noted was fiber depleted grain boundaries (Figure I.a., b, and c.) with the fibers having varying degrees of misalignment with respect to the growth direction. The second defect was a misalignment of groups of fibers with respect to each other resulting in a banded effect (Figure II.a., and b.).

The ultimate tensile strengths for the Al-Al_3Ni eutectic are shown as a function of temperature for the four growth rates in Figures III, IV, V, and VI. The tensile strengths of the 6.2 wt % Ni composite was greater than the 6.13 wt % Ni, the exceptions resulting from defects in microstructure. Figure VII demonstrates the comparative average tensile strengths at each growth rate as a function of temperature. The best overall growth rate for tensile strength at high temperature was found to be the 5.2 cm/hr rate.

Figure VIII demonstrates the contrast in the two configurations of stress-strain diagrams that were obtained

during testing. The tensile test specimens that are starred in the % elongation column in Appendix A were the particular samples that showed unusual elongation after yielding.

The results of the fiber count and interfiber spacing measurements are given in Figure IX. The slope of the interfiber spacing, (microns), versus the inverse square root of the growth rate, $R^{-\frac{1}{2}}$ $(cm/hr)^{-\frac{1}{2}}$, was determined to be 4.25×10^{-4} $cm^{3/2}hr^{-\frac{1}{2}}$. Photographs of the microstructures of the four growth rates are shown in Figure X.a., b., c., and d.

The results of the strain rate sensitivity test are tabulated in Table 1. The value of the strain rate sensitivity exponent, n, was found to be small, and it decreased with increasing % elongation.

TABLE I

MELT/ SPECIMEN #	GROWTH RATE	WT % Ni	% ELONGATION	n
3/62	6.9 cm/hr	6.2	2.45	0.1847
3/62	6.9 cm/hr	6.2	4.43	0.1172
3/64	9.4 cm/hr	6.2	4.04	0.231
3/64	9.4 cm/hr	6.2	6.08	0.1607

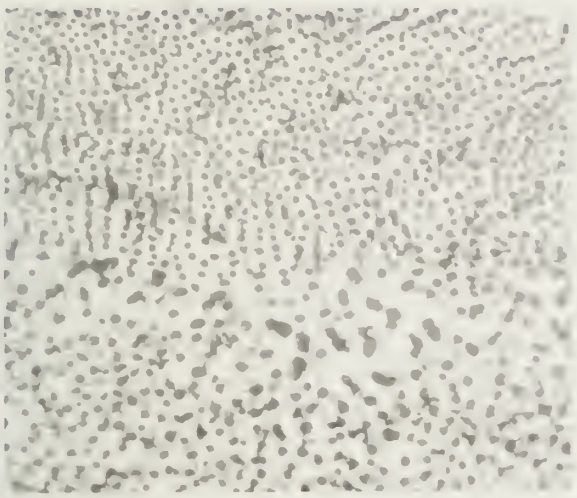

Figure I.a. Fiber depleted grain boundary, cross-section view. 900 x

Figure I.b. Fiber depleted grain boundaries, longitudinal view, with fractured fibers. 900 x

Figure I.c. Fiber depleted grain boundary, longitudinal view, with fractured fibers, missing sections removed in polishing. 900 x

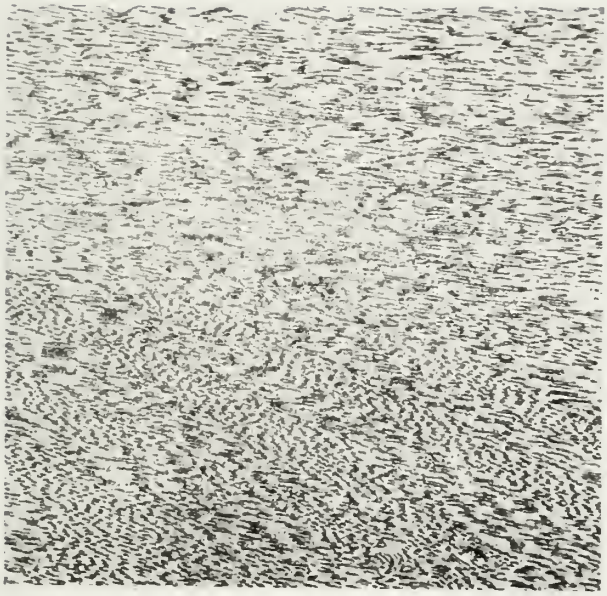

Figure II.a. Banded areas of misaligned fibers, no grain boundaries. 200 x

Figure II.b. Banded areas of misaligned fibers, no grain boundaries. 600 x

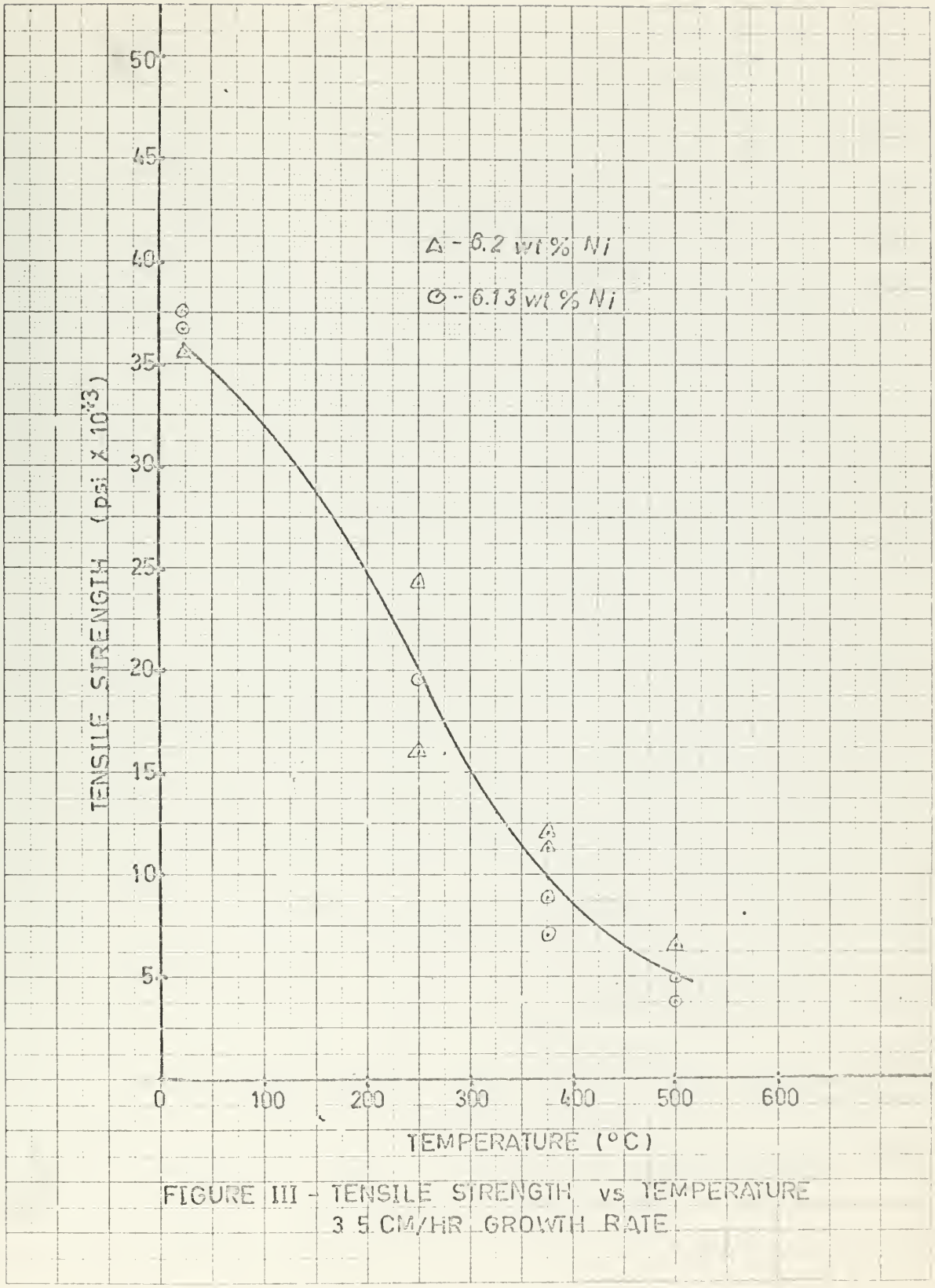

FIGURE III - TENSILE STRENGTH vs TEMPERATURE
3.5 CM/HR GROWTH RATE

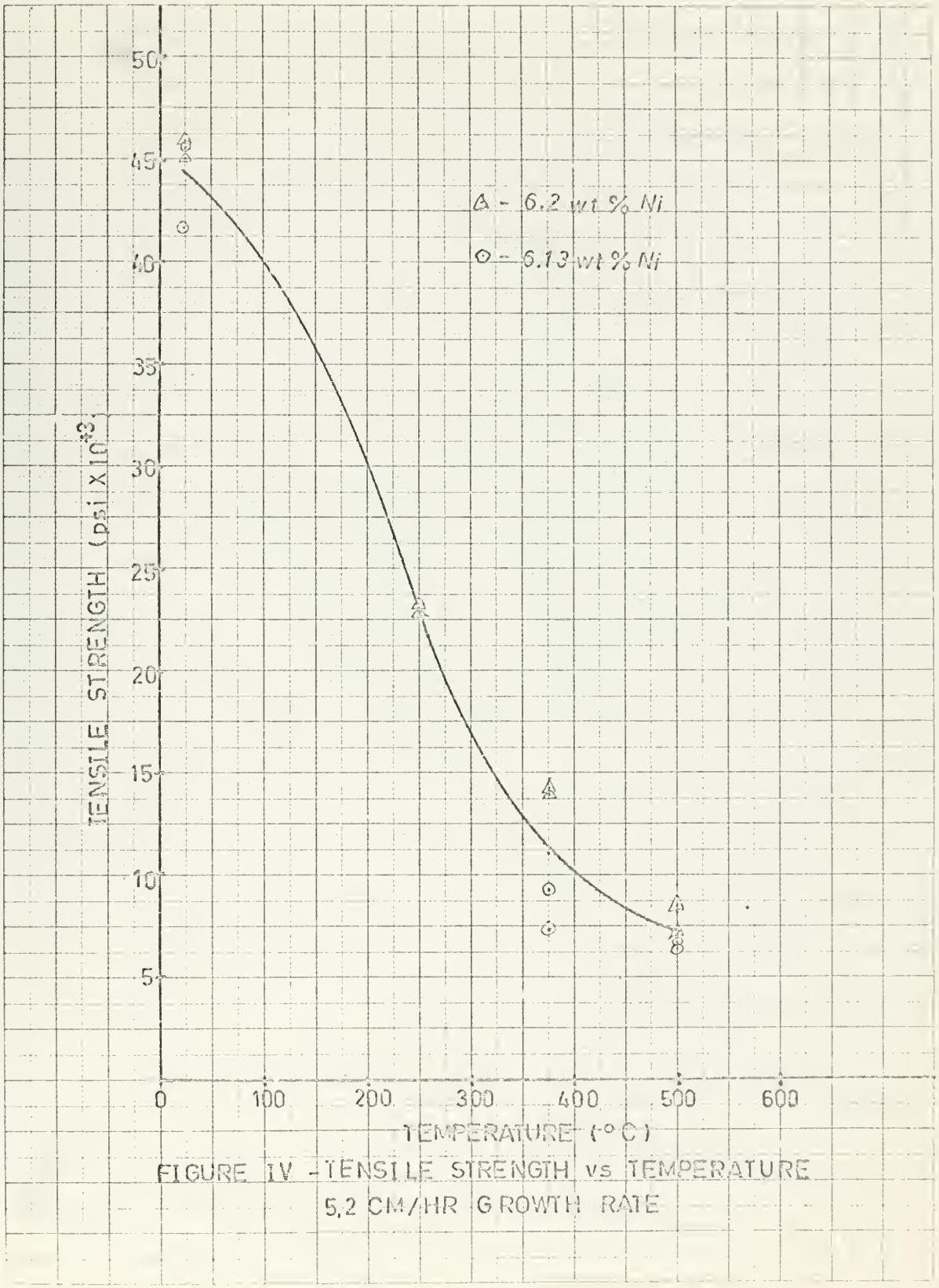

FIGURE IV - TENSILE STRENGTH vs TEMPERATURE
5.2 CM/HR GROWTH RATE

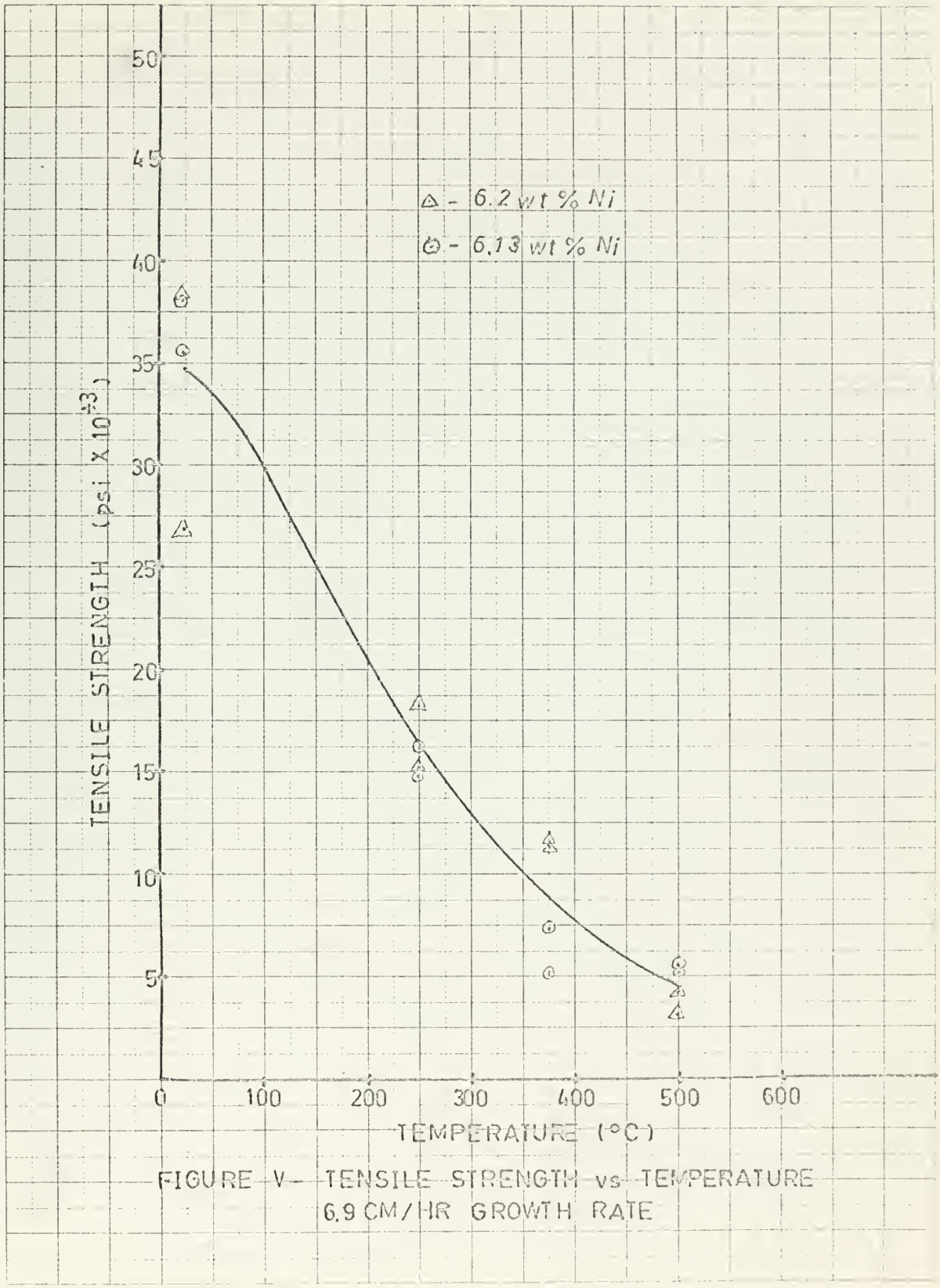

FIGURE V- TENSILE STRENGTH vs TEMPERATURE
6.9 CM/HR GROWTH RATE

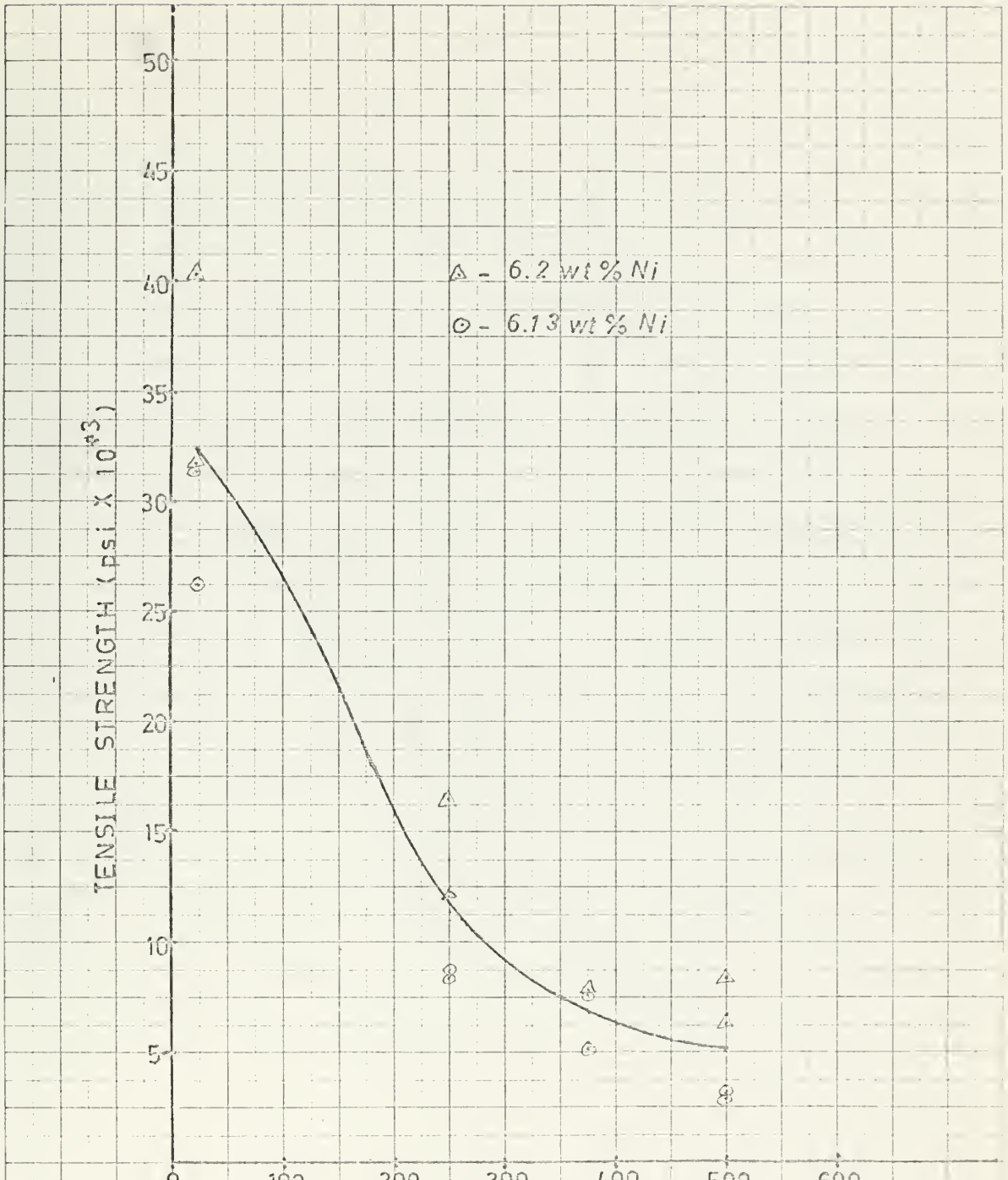

FIGURE VI - TENSILE STRENGTH vs TEMPERATURE
9.4 CM/HR GROWTH RATE

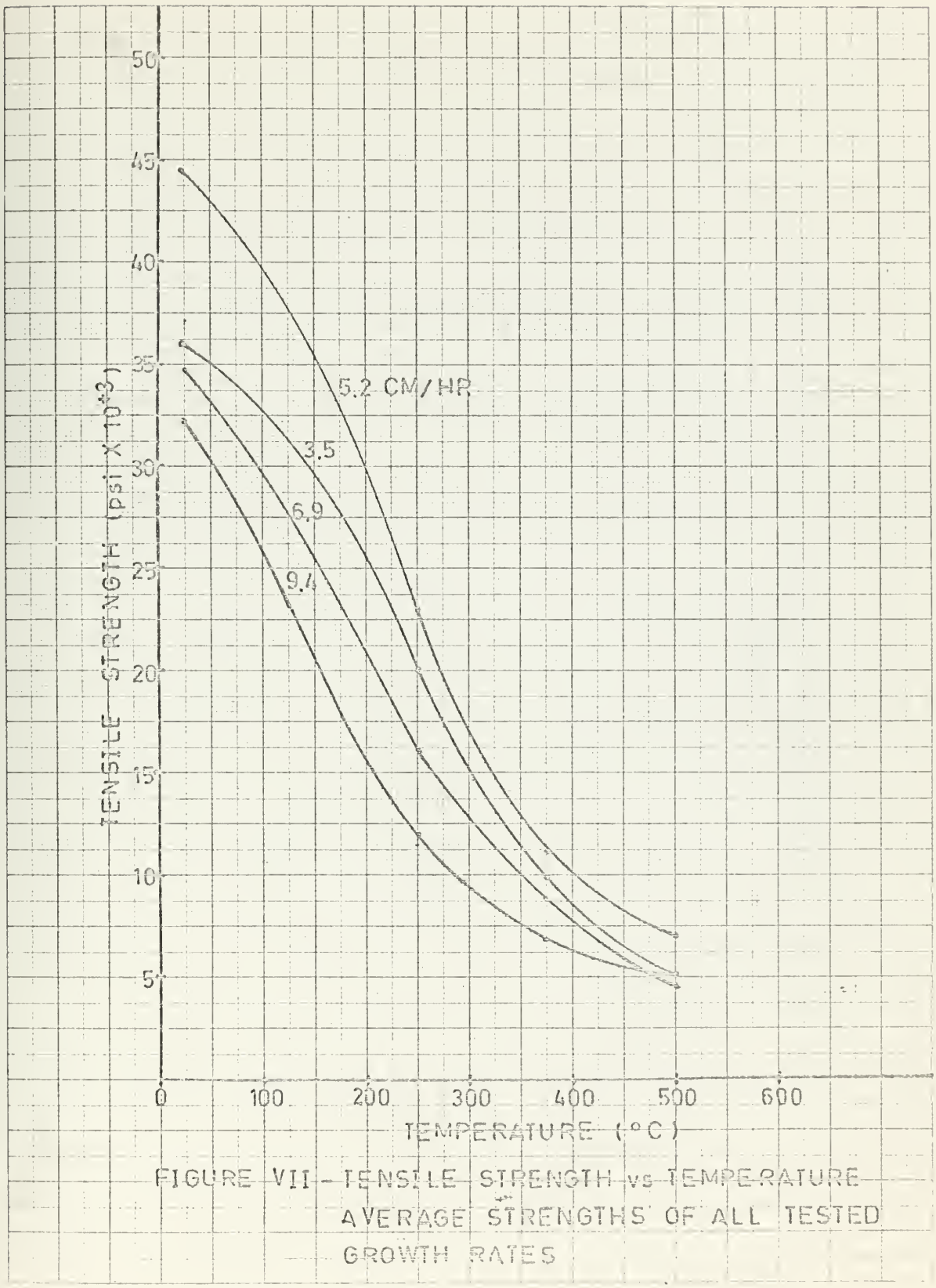

FIGURE VII - TENSILE STRENGTH vs TEMPERATURE
AVERAGE STRENGTHS OF ALL TESTED
GROWTH RATES

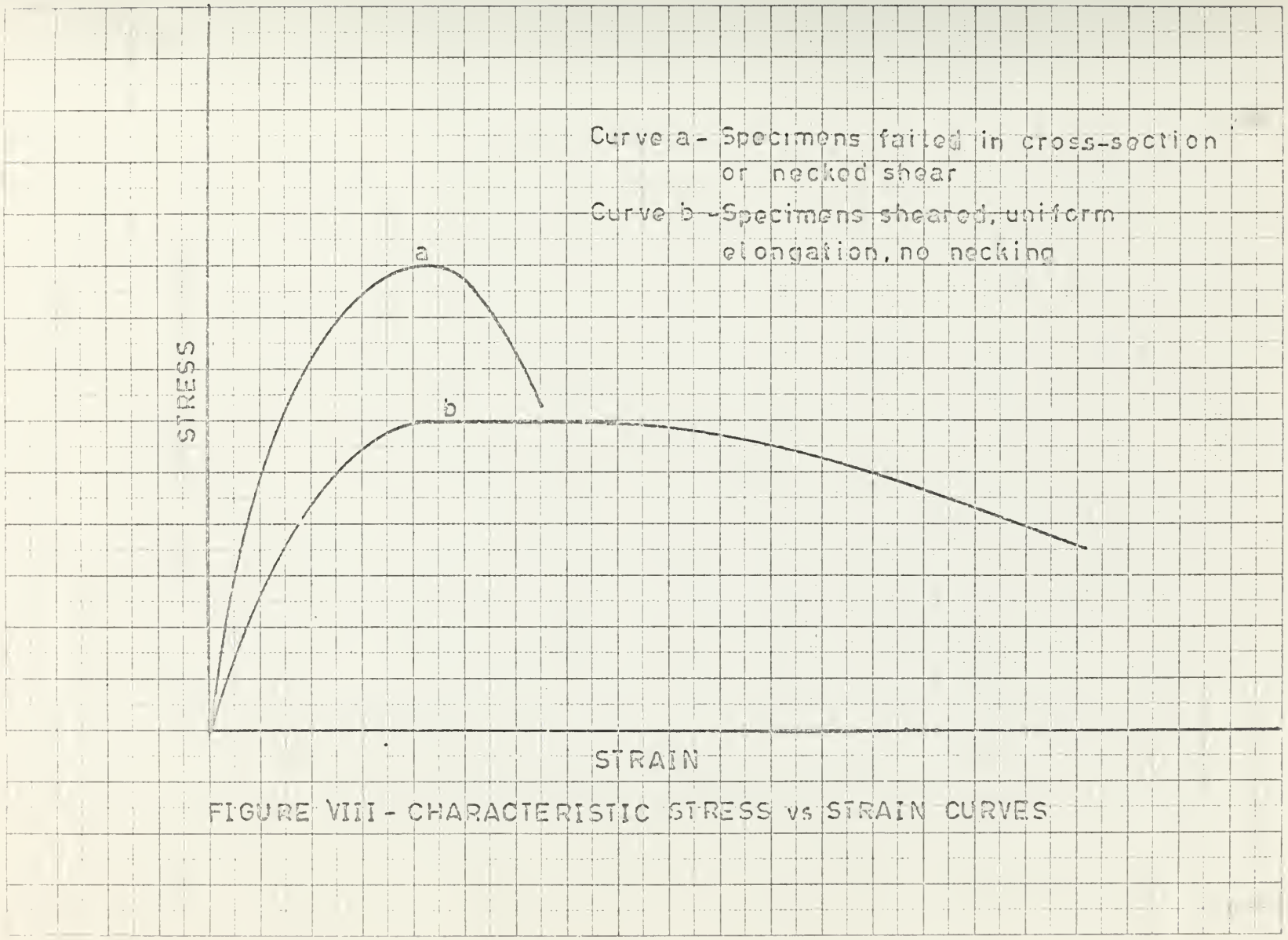

FIGURE VIII - CHARACTERISTIC STRESS vs STRAIN CURVES

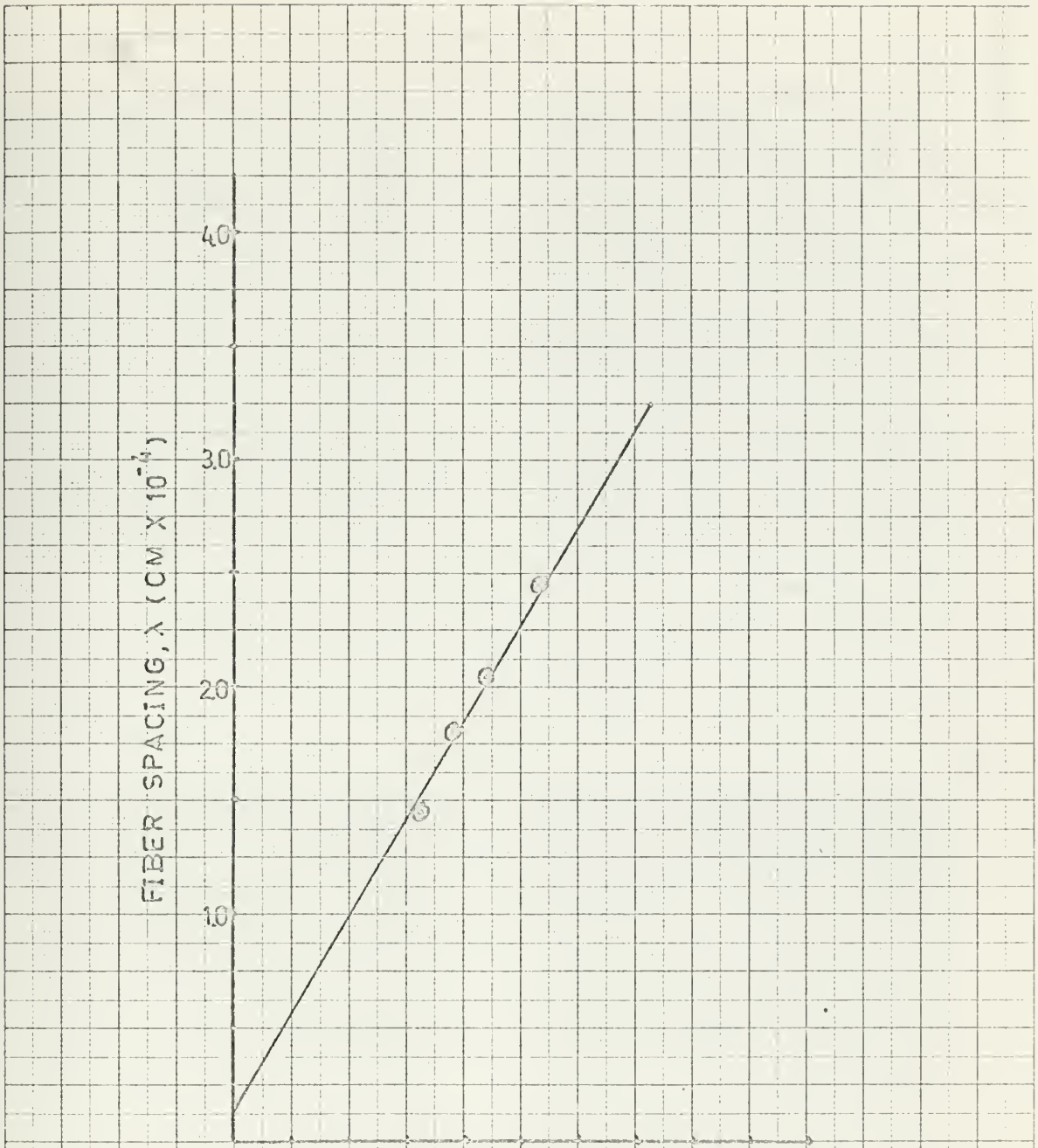

FIGURE IX - FIBER SPACING, λ, vs GROWTH RATE, $R^{-0.5}$

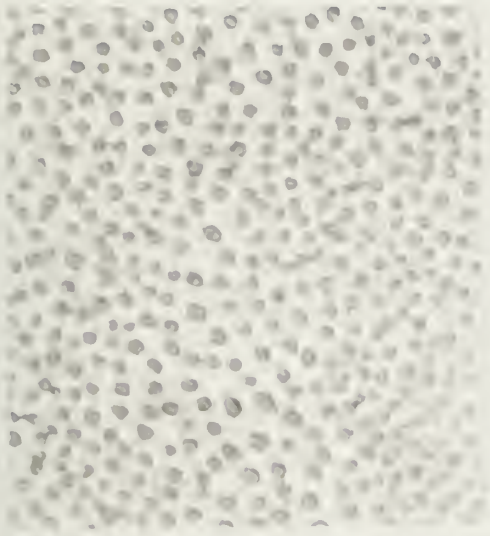

Figure X.a. 3.5 cm/hr growth rate, interfiber spacing. 1600 x

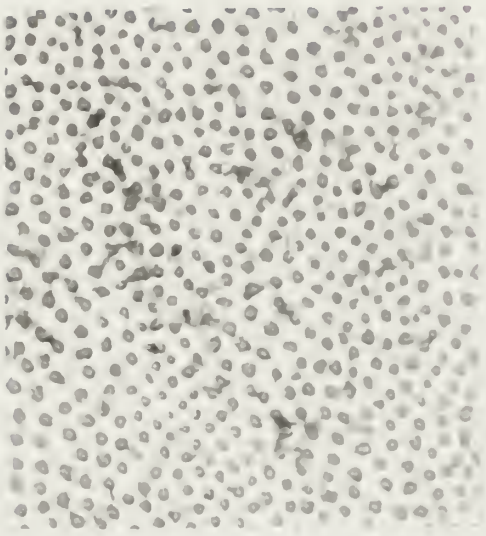

Figure X.b. 5.2 cm/hr growth rate, interfiber spacing. 1600 x

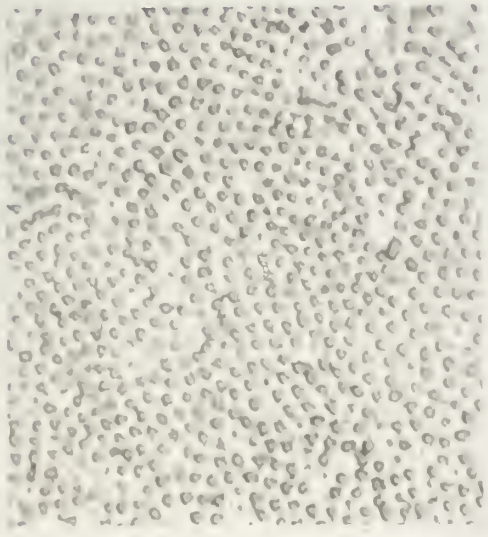

Figure X.c. 6.9 cm/hr growth rate, interfiber spacing. 1600 x

Figure X.d. 9.4 cm/hr growth rate, interfiber spacing. 1600 x

IV DISCUSSION OF RESULTS

A. FIBER SPACING

The measurement of fiber spacing for each growth rate was made by linear and area counts. The results shown in Figure IX are in good agreement with those of Hertzberg, Lemkey, and Ford.[7] As the solidification speed increased the eutectic Al_3Ni prefers the low surface energy rod formation. The fiber diameter and interfiber spacing becomes progressively finer as growth rate increases. Along the grain boundaries, however, considerable coarsening of structure takes place. In Figure I.a., b., and c., these coarse fibers can be seen in both the cross-sectional and longitudinal views. In Appendix A, the tabulation data includes the number of grains that were counted in the cross section of those specimens that were microscopically examined. The general trend of the observations is that the number of grains in the cross section tends to increase with increasing solidification rate. As will be discussed later it is believed that transient distrubances in the solidification process do not damp out at the higher growth rates.

B. ROOM TEMPERATURE TENSILE STRENGTH

Although the strongest specimens were equivalent in strength in this investigation to the results reported by

Hertzberg, Lemkey, and Ford;[7] the average tensile strengths at room temperature do not compare favorably. In the earlier work, it was found that the tensile strength increased with increasing solidification rate in the range covered by this investigation. They also found, however, that defective microstructures considerably reduced the tensile strength of the composite, in agreement with the present work.

C. VARIATION OF WT % Ni IN THE COMPOSITE

Composites containing 6.13 and 6.2 wt % Ni were directionally solidified to investigate the effect of nickel content on tensile strength. The range of eutectic composition as reported by Lemkey, Hertzberg, and Ford[6] is 6.18 ± 0.05 wt % Ni. The results demonstrate that the higher percentage nickel composite had the same tendency to solidify with more grains as the growth rate was increased. The 6.2 wt % Ni specimens, however, were generally stronger both at room and high temperatures (see Figures III, IV, V, and VI).

D. TENSILE STRENGTH AT ELEVATED TEMPERATURE AND ITS DEPENDENCY ON MICROSTRUCTURE

As the temperature of the tensile tests was increased, the average tensile strengths decreased rapidly (see Figure VII). Above 250°C, however, the strengths leveled off. At each temperature and growth rate there was considerable scatter in the results; therefore the average

tensile strenths are not necessarily representative of the composites' actual behavior.

The first group of 250°C test specimens examined were numbers 1/17, 3/25, and 3/26, which were grown at 3.4 cm/hr. Number 1/17 failed with a jagged cross-sectional break (see Appendix A., Figure XIII) and exhibited good strength. Three grains were counted in the cross section; however, the fibers were well aligned on both sides of the grain boundaries. This was the only specimen in which broken fibers within the grains (not at grain boundaries) were in evidence (see Figure XI). Sample number 3/25, which failed with a cross section (cone) break, had the highest strength of the three. There were no grain boundaries in its cross section, and the alignment of the fibers longitudinally was excellent. Specimen number 3/26 had two grains in its cross section, and it failed in jagged matrix shear. Figure XII demonstrates the multiple shear planes of the jagged shear failure. The entire left portion shown in the figure has sheared in a plane parallel to the actual failure plane. The fibers can be seen to have been bent in the lower right hand corner, in order to align themselves parallel to the shear plane. The overall alignment was excellent on both sides of the grain boundaries. Although there were no broken fibers within the grains, the coarse fibers in the grain boundaries had fractured (see Figure I.b and c.).

Figure XI. Fractured fibers, not at grain boundary. 900 x

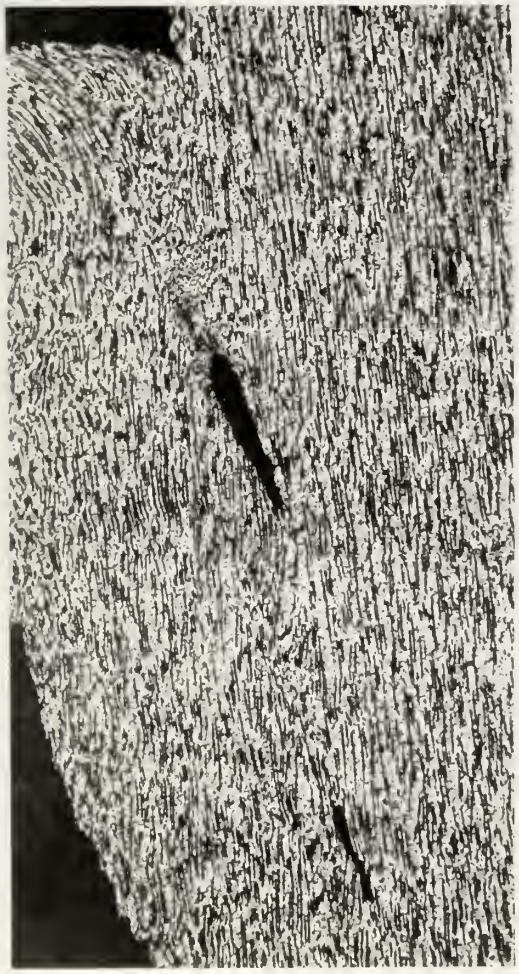

Figure XII. Secondary shear failure plane parallel to shear fracture plane. 150 x

Specimens number 1/20, 3/27, and 3/28 were examined in the 5.2 cm/hr growth rate group. Number 1/20 failed at the threaded grip so its strength is not plotted in Figure IV. The alignment of fibers in all three samples was excellent, and there were no grain boundaries in the cross sections. Specimen numbers 3/27 failed in cross section (cone), whereas number 3/28 failed in jagged cross section. The microstructure of 3/28 indicates that failure commenced in matrix shear. The shear line, however, was halted by fiber intervention, and the sample then failed in cross section.

The microstructures of the 6.9 and 9.4 cm/hr growth rate material demonstrate the effect of the number of grains in the cross section and fiber misalignment on the type of fracture and strength characteristics of the composite. Specimens number 2/21 and 3/29 had one and two grains in their cross sections respectively, and both failed in jagged cross section. In samples number 2/22, 2/23, 2/24, 3/30, 3/31, and 3/32, however, all had four or more grains in their cross sections, and they all failed in matrix shear. Whereas the fiber misalignment between grains was less than ten degrees in the samples that failed with a cross section break, the maximum misalignment in the shear failure samples ranged from ten degrees in sample 3/32 to thirty degrees in samples 2/24, 3/30, and 3/31. In addition, all the shear failure

samples had fractured coarse fibers at the grain boundaries, both at and away from the sheared surface. It therefore appears that the mode of failure and the ultimate tensile strength is directly dependent on the number of grains in the cross section, and the maximum angle of misorientation of the fibers.

Possible reasons for the defective microstructure are as follows:

a. vibrations during growth--although the directional solidification furnace was shock mounted on rubber pads, vibrations from room traffic could have been transmitted to the carbon boat. Simultaneously, vibrations could have affected the counter weight system of the drive gearing, causing fluctuations in the DC motor drive speed.

b. heat transfer--changes in the flow rates of argon gas through the Vycor tube and the chill water to the heat sink may have varied the convective heat transfer characteristics during solidification.

c. tool markings--a pointed cutting tool was used when the carbon boat was turned on a lathe. The resulting tool markings evidently provided nucleation cites for solidification. As mentioned previously in the experimental procedure, the bottom section of all rods at all growth rates was found to be multigrained with banded

misoriented fibers. At slow growth rates the microstructural defects were largely eliminated after ½ to 3/4 " of growth. At the higher rates, however, the growth defects continued over the entire length.

Any one or combination of the above possibilities would have been sufficient to cause irregular growth.

E. ELONGATION PHENOMENA

The normal stress vs strain characteristics are typified by curve "a" of Figure VIII. After reaching the ultimate strength at between 1 and 3% elongation, the stress dropped off sharply to zero. Some of the specimens, however, showed considerable elongation after yielding. In Appendix A the values given under % elongation are those at which the specimens reached their ultimate tensile strength. All samples that showed large elongation after yield are starred with an asterisk after the elongation figure.

The microstructures of specimens number 2/54, 2/55, 3/63, and 3/64 were examined to determine the cause of the unusual elongation. The specimens were also examined immediately after testing to determine general differences in fracture. The sharp drop in stress in curve "a" of Figure VIII was characteristic of specimens that failed in both shear and tensile cross section. The shear failure specimens, however, did not elongate uniformly

over the gage length; necking occurred in the fracture area. Specimen number 3/63, which failed in tensile cross section, had two grains in its cross section. The fibers were well aligned, and no broken coarse fibers were seen in the grain boundary.

The specimens that had large elongation after yield all failed in matrix shear. Investigation of the failed samples showed that the gage section had elongated uniformly. Chevron markings were in evidence where the matrix had failed in shear away from the final fracture. Study of the microstructures of specimens number 2/54, 2/55, and 3/64 revealed shear lines parallel to the fracture surface where the fiber ends had turned slightly to align themselves with the shear line (Figure XII). The specimens had a number of fiber depleted grain boundary regions where the coarse fibers had fractured. Across the grain boundaries, the fibers were well aligned in specimens 3/63 and 3/64. The increased strength and uniform elongation along the gage length of these two samples indicate that the fibers were misaligned with respect to the tensile axis. The fibers in specimens 2/54 and 2/55 were misaligned across the grain boundaries by 15° and 10° respectively.

Although the fibers provide considerable resistance to matrix shear, the combination of fiber misalignment and

fiber depleted grain boundaries allows uniform deformation in parallel shear planes along the gage length.

F. STRAIN RATE SENSITIVITY

The strain rate sensitivity tests (Table I) showed that the strain rate sensitivity exponent was low. The fiber composite, therefore, has little tendency for superplastic deformation. With increasing elongation, the strain rate sensitivity exponent decreased.

V CONCLUSIONS

1. The interfiber spacing decreases linearly with the inverse square root of the growth rate. The sensitivity of the composite to disturbances during solidification increases with increasing growth rate. At higher growth rates, disturbances do not damp out, resulting in defective microstructure.
2. With increasing temperature, the tensile strength of the composite decreases rapidly and then levels off after 250°C. Strength increases with growth rate from 3.5 to 5.2 cm/hr. The microstructural defects encountered in specimens grown in excess of 5.2 cm/hr do not permit a proper evaluation of the sample strength characteristics.
3. The 6.13 and 6.2 wt % Ni composites were both prone to defective microstructure at the higher growth rates. The maximum tensile strength of the 6.2 wt % Ni specimens, however, was considerably higher than the specimens with smaller nickel content, for all temperatures and growth rates tested.
4. Tensile specimens that fail in either jagged cross section or symmetrical cross section are indicative of good fiber alignment and few grains. Specimens that fail in matrix shear with high tensile strengths

indicate good fiber alignment but at an angle to the tensile axis. A defective microstructure, however, results in (1) matrix shear at low ultimate strength, and (2) broken coarse fibers at fiber depleted grain boundaries.

5. Defective microstructures are believed to be the result of (1) vibration transmission to the carbon boat, (2) heat transfer fluctuations, and (3) nucleation cites at the base of the carbon boat, left after machining. At lower growth rates these effects are overcome and largely disappear. At higher growth rates, however, defective growth continues throughout the length.
6. Unusual uniform elongation over the gage length is a high temperature characteristic of specimens that combine multiple grains with misaligned fibers. Although the Al_3Ni fibers interfere with matrix shear, the combination of fiber depleted grain boundaries and misaligned fibers allows parallel shear planes to occur throughout the gage length.
7. The composite does not deform superplastically in the temperature range up to 500°C. As the percent elongation increases, the strain rate sensitivity index decreases, at small values.

VI RECOMMENDATIONS

Since a uniform microstructure was difficult to attain at higher growth rates, the actual cause of the defects should be investigated.

1. Steady state and transient effects on microstructure of known changes in flow rate of cooling water and argon gas (in the absence of all vibrations) should be investigated along the length of rods directionally solidified at various growth rates.
2. Vibrations of known energy and frequency could be induced at the furnace frame (in the absence of heat transfer disturbances), and measurements made of their effects on microstructure in the same manner as above.

VII APPENDIX

A. TABULTATION OF DATA

1. All Specimens Tensile Tested

MELT/ SPECIMEN	R	Wt % Ni	T	σ(psi)	ε %	TYPE FRACTURE (FIGURE XIII)
1/1	3.5	6.13	22	36700	2.11	Cross section (cone)
1/2	3.5	6.13	22	37600	2.08	Shear
1/3	5.2	6.13	22	45600	2.04	Cross section (jagged)
1/4	5.2	6.13	22	41700	2.0	Shear
2/5	6.9	6.13	22	35500	2.55	Shear (jagged)
2/6	6.9	6.13	22	38100	2.45	Cross section (cone)
2/7	9.4	6.13	22	26200	2.46	Shear
2/8	9.4	6.13	22	31300	2.75	Shear (jagged)
3/9	3.5	6.2	22	35500	1.65	Cross section (jagged)
3/11	5.2	6.2	22	45800	1.16	Cross section (jagged)
3/12	5.2	6.2	22	45000	1.10	Shear (jagged)
3/13	6.9	6.2	22	-----	----	Grip failure
3/14	6.9	6.2	22	26900	1.0	Cross section (jagged)
3/15	9.4	6.2	22	31700	1.26	Shear
3/16	9.4	6.2	22	40300	1.2	Cross section (jagged)
1/17	3.5	6.13	250	19600	2.03	Cross section (jagged)
1/20	5.2	6.13	250	-----	----	Grip failure
2/21	6.9	6.13	250	14800	2.85	Cross section (jagged)
2/22	6.9	6.13	250	16280	2.82	Shear (jagged)
2/23	9.4	6.13	250	8400	2.38*	Shear
2/24	9.4	6.13	250	8700	2.59*	Shear

MELT/ SPECIMEN	R	Wt % Ni	T	σ(psi)	ε%	TYPE FRACTURE (FIGURE XIII)
3/25	3.5	6.2	250	24300	3.11	Cross section (cone)
3/26	3.5	6.2	250	16000	3.09	Shear
3/27	5.2	6.2	250	22800	2.93	Cross section (cone)
3/28	5.2	6.2	250	23100	2.91	Cross section (jagged)
3/29	6.9	6.2	250	18200	2.89	Cross section (cone)
3/30	6.9	6.2	250	15100	2.79	Shear
3/31	9.4	6.2	250	12100	2.71	Shear
3/32	9.4	6.2	250	16500	3.0	Shear
1/33	3.5	6.13	375	7100	1.93*	Shear (jagged)
1/34	3.5	6.13	375	8900	3.07*	Shear (jagged)
1/36	5.2	6.13	375	9300	2.61*	Shear
2/37	6.9	6.13	375	7400	2.52*	Shear
2/38	6.9	6.13	375	5200	1.9*	Shear
2/39	9.4	6.13	375	5100	1.78	Shear
2/40	9.4	6.13	375	7700	2.64	Cross section (jagged)
3/41	3.5	6.2	375	12000	2.49	Shear (jagged)
3/42	3.5	6.2	375	11400	2.44	Shear (jagged)
3/43	5.2	6.2	375	13900	3.13	Cross section (jagged)
3/44	5.2	6.2	375	14100	2.79	Cross section (cone)
3/45	6.9	6.2	375	11400	2.8	Cross section (cone)
3/46	6.9	6.2	375	11450	2.41	Shear (jagged)
3/47	9.4	6.2	375	7800	2.59	Shear (jagged)
1/49	3.5	6.13	500	3500	1.62	Shear
1/50	3.5	6.13	500	5000	2.49	Cross section (cone)
1/51	5.2	6.13	500	6400	2.62	Shear

MELT/ SPECIMEN	R	Wt % Ni	T	σ(psi)	ε %	TYPE FRACTURE (FIGURE XIII)
1/52	5.2	6.13	500	6500	2.43	Shear
2/53	6.9	6.13	500	5500	2.4	Shear
2/54	6.9	6.13	500	5100	2.09	Shear
2/55	9.4	6.13	500	3000	2.55*	Shear
2/56	9.4	6.13	500	3200	2.99*	Shear
3/57	3.5	6.2	500	6600	2.36	Cross section (jagged)
3/59	5.2	6.2	500	7100	2.2	Shear (jagged)
3/60	5.2	6.2	500	8600	2.93	Cross section (cone)
3/61	6.9	6.2	500	3100	2.14*	Shear
3/62	6.9	6.2	500	4300	2.13*	Shear
3/63	9.4	6.2	500	8400	3.1	Cross section (cone)
3/64	9.4	6.2	500	6300	2.65*	Shear (jagged)

*Unusually large elongation after yield.

2. Microstructure Survey

MELT/ SPECIMEN	R cm/hr	# GRAINS X-SECTION	COMMENTS
1/17	3.5	3	Good fiber alignment some broken fibers (not at grain boundaries).
1/20	5.2	1	Excellent fiber alignment.
2/21	6.9	1	Misalignment about 10°, fiber ends bent at fracture surface.
2/22	6.9	7	Misalignment about 30°, broken coarse fibers along grain boundaries.
2/23	9.4	5	Misalignment about 20°, broken coarse fibers along grain boundaries.
2/24	9.4	5	Misalignment about 30°, broken coarse fibers.
3/25	3.5	1	Excellent fiber alignment.
3/26	3.5	2	Excellent fiber alignment, fiber ends bent slightly at fracture surface and at second shear plane parallel to fracture.
3/27	5.2	1	Excellent fiber alignment.
3/28	5.2	1	Excellent fiber alignment, started to fail in matrix shear.
3/29	6.9	2	Good fiber alignment, no broken fibers noticed.
3/30	6.9	7	Misalignment about 30°, broken coarse fibers at grain boundaries.
3/31	9.4	4	Same as above.
3/32	9.4	5	Misalignment about 10°, broken fibers at grain boundaries.
2/54	6.9	5	Misalignment about 15°, few broken fibers at grain boundaries.

MELT/ SPECIMEN	R cm/hr	# GRAINS X-SECTION	COMMENTS
2/55	9.4	8	Misalignment about 10°, considerable grain boundary area with broken fibers.
3/63	9.4	2	Good alignment except at apex of cone where fibers changed direction, possible misalignment with tensile axis.
3/64	9.4	2	Good alignment, broken fibers at grain boundary.

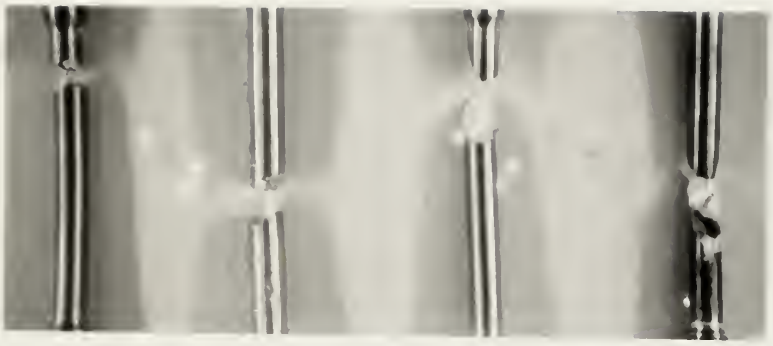

Figure XIII. Characteristic modes of failure. From left: cross-section (cone); cross-section (jagged); shear; and shear (jagged).

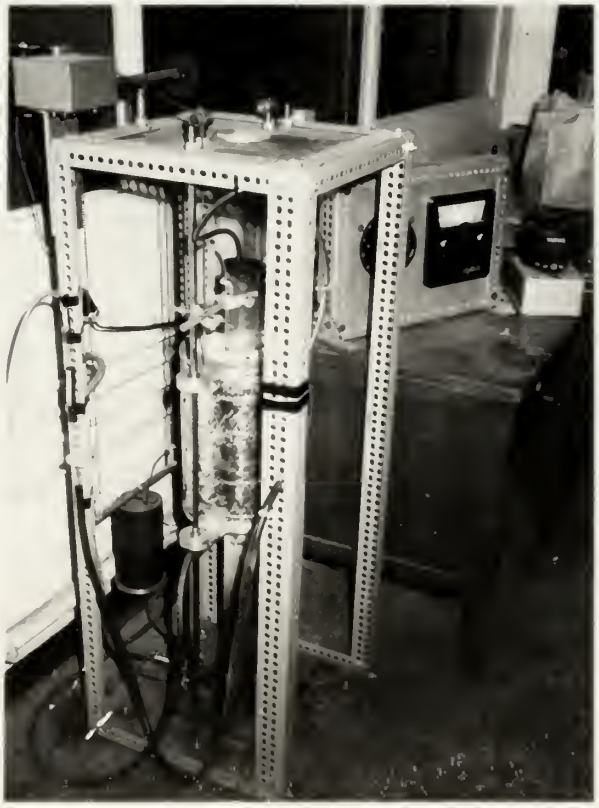

Figure XIV. Directional solidification furnace.

B. DESCRIPTION OF APPARATUS

1. Unidirectional Solidification Equipment (Figure XIV) and its associated speed and temperature controls.

The furnace used for the directional solidification of the composite was built by R. Render, W. Marsh, and the author. The heating element consisted of two sets of resistance coils mounted vertically and connected in parallel. The rated capacity of each set was 9 amperes at 115 volts, 60 cps, 1000°C. The internal diameter and length of the cylindrical elements was 3.5 and 12 inches respectively. Insulation for the furnace consisted of the following:

(a) Vermiculite between an eight inch diameter stainless steel sheetmetal cylinder and the heating elements.

(b) Insulating jacket on the outside of the stainless steel cylinder consisted of two layers of aluminum foil, two layers of asbestos cloth, and one layer of spun glass.

(c) $\frac{1}{2}$" transite spacers between the heating elements and the aluminum end plates.

A temperature control thermocouple was located at the middle of the twelve inch heating element. To prevent failure of the heating elements, a variac and an ammeter were installed in the controller circuitry. During solidification the current was limited to 6.5 amperes to each

heating coil. The temperature at the base of the carbon boat was monitored by a thermocouple located one inch above the chill water heat sink.

Rectified AC power was supplied through a variac to the DC drive motor. The motor was rated at 115 volts, 1200 RPM. By adjusting the terminal voltage to the drive motor, the verticle growth rate could be regulated in the range of 2-10 cm/hr.

Atmosphere control was accomplished by evacuating the Vycor cylinder and then purging it with welding grade argon. This procedure was done three times; after which a positive pressure of argon was maintained in the Vycor cylinder to prevent oxygen contamination.

At the end of a solidification run, the furnace and motor drive units were shut off by a microswitch.

2. Temperature Control and Monitoring Equipment - Tensile Test.

The furnace and its temperature controls were built by R. Render. The heating elements were two half-cylinder resistance coils, twelve inches long, with an inner radius of 0.75 inches. The coils were installed in a sheetmetal cylinder which was cut in half lengthwise and hinged. Between the heating elements and the metal cylinder halves, firebrick was fitted for insulation. The clamshell furnace permitted easy access to the Instron grips for installing and removing test samples. The two hinged halves were

clamped together during a test run. For temperature control and monitoring, two thermocouples were placed in receptacles on the upper grip. The temperature control electrical connections were the same as those for the directional growth furnace.

VIII BIBLIOGRAPHY

1. K. A. Jackson and J. D. Hunt: Trans. Met. Soc. AIME, 1966, Vol. 236, pp. 1129-1142.
2. J. D. Hunt and K. A. Jackson: Trans. Met. Soc. AIME, 1967, Vol. 239, pp 864-867.
3. F. R. Mollard and M. C. Flemings: Trans. Met. Soc. AIME, 1967, Vol. 239, pp 1526-1546.
4. R. W. Kraft and D. L. Albright: Trans. Met. Soc. AIME, 1961, Vol. 221, pp 95-102.
5. W. A. Tiller: Liquid Metals and Solidification, pp 276-318, ASM, Cleveland, Ohio (1958).
6. F. D. Lemkey, R. W. Hertzberg and J. A. Ford: Trans. Met. Soc. AIME, 1965, Vol. 233, pp 334-341.
7. R. W. Hertzberg, F. D. Lemkey and J. A. Ford: Trans. Met. Soc. AIME, 1965, Vol. 233, pp 342-354.
8. M. Salkind, F. George, F. Lemkey and B. J. Bayles: Final Report, Contract NOW 65-0384-d, United Aircraft Research Laboratories, May 1966.
9. F. D. George, J. A. Ford and M. J. Salkind: The Effect of Fiber Orientation and Morphology on the Tensile Behavior of Al_3Ni Whisker Reinforced Aluminum, ASTM Symp. on Metal Matrix Composites, June 1967.
10. B. J. Bayles, J. A. Ford, and M. J. Salkind: Trans. Met. Soc. AIME, 1967, Vol. 239, pp 844-849.

11. A. Kelly and G. J. Davies: Met. Rev., 1965, Vol. 10, No. 37, pp 36-41.